Am. J. Hum. Genet. 73:233–246, 2003

Mutations in Novel Peroxin Gene *PEX26* That Cause Peroxisome-Biogenesis Disorders of Complementation Group 8 Provide a Genotype-Phenotype Correlation

Naomi Matsumoto,[1,*] Shigehiko Tamura,[1,*] Satomi Furuki,[1,*] Non Miyata,[1] Ann Moser,[2] Nobuyuki Shimozawa,[3] Hugo W. Moser,[2] Yasuyuki Suzuki,[3] Naomi Kondo,[3] and Yukio Fujiki[1,4]

[1]Department of Biology, Faculty of Sciences, Kyushu University Graduate School, Fukuoka, Japan; [2]Department of Neurology and Pediatrics, Kennedy-Krieger Institute, Johns Hopkins University, Baltimore; [3]Department of Pediatrics, Gifu University School of Medicine, Gifu, Japan; and [4]SORST, Japan Science and Technology Corporation, Kawaguchi, Saitama, Japan

The human disorders of peroxisome biogenesis (PBDs) are subdivided into 12 complementation groups (CGs). CG8 is one of the more common of these and is associated with varying phenotypes, ranging from the most severe, Zellweger syndrome (ZS), to the milder neonatal adrenoleukodystrophy (NALD) and infantile Refsum disease (IRD). *PEX26*, encoding the 305-amino-acid membrane peroxin, has been shown to be deficient in CG8. We studied the *PEX26* genotype in fibroblasts of eight CG8 patients—four with the ZS phenotype, two with NALD, and two with IRD. Catalase was mostly cytosolic in all these cell lines, but import of the proteins that contained PTS1, the SKL peroxisome targeting sequence, was normal. Expression of *PEX26* reestablished peroxisomes in all eight cell lines, confirming that *PEX26* defects are pathogenic in CG8 patients. When cells were cultured at 30°C, catalase import was restored in the cell lines from patients with the NALD and IRD phenotypes, but to a much lesser extent in those with the ZS phenotype, indicating that temperature sensitivity varied inversely with the severity of the clinical phenotype. Several types of mutations were identified, including homozygous G89R mutations in two patients with ZS. Expression of these *PEX26* mutations in *pex26* Chinese hamster ovary cells resulted in cell phenotypes similar to those in the human cell lines. These findings confirm that the degree of temperature sensitivity in *pex26* cell lines is predictive of the clinical phenotype in patients with *PEX26* deficiency.

Introduction

Peroxisomes are single-membrane–bounded ubiquitous organelles present in a wide variety of eukaryotic cells. The significance of peroxisomal function is highlighted by the severity of clinical manifestations of the human genetic peroxisome-biogenesis disorders (PBDs [MIM 601539]), in which various metabolic pathways, such as β oxidation of very-long-chain fatty acids and the synthesis of plasmalogens (van den Bosch et al. 1992), are impaired. The PBDs include Zellweger syndrome (ZS [MIM 214100]), neonatal adrenoleukodystrophy (NALD [MIM 202370]), infantile Refsum disease (IRD [MIM 266510]), and rhizomelic chondrodysplasia punctata (RCDP [MIM 215100]) (Lazarow and Moser 1995). Patients with ZS have severe nervous-system deficits and characteristic dysmorphic features and rarely live beyond the 1st year. Patients with NALD and IRD have abnormalities that resemble ZS but are less severe. The three disorders are now considered to form a clinical continuum, with ZS the most severe, NALD intermediate, and IRD the least severe. Patients with NALD and IRD survive to early childhood and occasionally to the 3rd decade or later (Lazarow and Moser 1995). Patients with RCDP show distinct phenotypic characteristics, such as severe growth failure and rhizomelia. Genetic heterogeneity consisting of 12 complementation groups (CGs) has been identified in PBDs (Fujiki 2000; Ghaedi et al. 2000; Matsumoto et al. 2001). The primary cause for PBDs is the impaired biogenesis of peroxisomes (Fujiki 2000; Gould and Valle 2000).

Import of peroxisomal matrix proteins is mediated by two types of peroxisomal targeting signals (PTSs): the C-terminal uncleavable tripeptide PTS1, -S/A/C-K/R/H-L/(M), identified in many enzymes (e.g., acyl-CoA oxidase [AOx]); and the cleavable nonapeptide presequence PTS2, -(R/K)(L/V/I)X_5(H/Q)(L/A)- ("X" denotes

Received February 12, 2003; accepted for publication May 7, 2003; electronically published July 8, 2003.

Address for correspondence and reprints: Dr. Yukio Fujiki, Department of Biology, Faculty of Sciences, Kyushu University Graduate School. 6-10-1 Hakozaki, Higashi-ku, Fukuoka 812-8581, Japan. E-mail: yfujiscb@mbox.nc.kyushu-u.ac.jp

Nucleotide sequence data reported herein are available in the DDBJ/EMBL/GenBank databases; for details, see the Electronic-Database Information section of this article.

* The first three authors contributed equally to this work.

© 2003 by The American Society of Human Genetics. All rights reserved.
0002-9297/2003/7302-0003$15.00

any amino acid), located at the N-terminus in proteins (e.g., 3-ketoacyl-CoA thiolase [hereafter referred to as "thiolase"]).

We previously isolated 13 CGs of peroxisome-biogenesis–defective Chinese hamster ovary (CHO) cell mutants, including ZP167 of CG8 (Ghaedi et al. 1999), mostly by the 9-(1′-pyrene)nonanol (P9OH)/UV selection method (Morand et al. 1990; Shimozawa et al. 1992). All CHO cell mutants resembled fibroblasts from patients with PBDs in that they showed defects in peroxisome assembly, despite normal synthesis of peroxisomal proteins. Complementation studies showed that 10 of the mutants corresponded to 10 of the 12 human CGs, whereas 3 were distinct (Fujiki 2000; Ghaedi et al. 2000). We have so far isolated or identified nine peroxin cDNAs—including *PEX1, PEX2, PEX3, PEX5, PEX6, PEX7, PEX12, PEX14,* and *PEX19*—by genetic strategies, such as functional phenotype-complementation assays using CHO cell mutants (Fujiki 2000; Mukai et al. 2002). Furthermore, 11 *PEX* genes required for peroxisome biogenesis—*PEX1, PEX2, PEX3, PEX5, PEX6, PEX7, PEX10, PEX12, PEX13, PEX16,* and *PEX19*—have been demonstrated as the genetic cause responsible for PBD CGs: CG1 (CG-E), CG10 (CG-F), CG12 (CG-G), CG2, CG4 (CG-C), CG11 (CG-R), CG7 (CG-B), CG3, CG13 (CG-H), CG9 (CG-D), and CG14 (CG-J), respectively (with the U.S./European and Japanese names, the latter given in parentheses) (Fujiki 2000; Ghaedi et al. 2000; Gould and Valle 2000; Matsumoto et al. 2001; Mukai et al. 2002).

Only the genetic cause for CG8 (CG-A) PBDs had remained unidentified for over a decade. Very recently, we have isolated the novel peroxin Pex26p cDNA, encoding 34-kDa peroxisomal membrane protein, by a genetic phenotype-complementation cloning strategy using a CHO cell mutant, ZP167 of CG8 (Matsumoto et al. 2003). *PEX26* expression also complemented the impaired catalase import in fibroblasts from a CG8 patient with NALD. However, molecular and biochemical defects in peroxisome biogenesis that underlie the difference in severity between the CG8 PBDs (ZS, NALD, and IRD) remained undefined. In the present study, we report that the import of catalase and PTS2 proteins, such as thiolase, is temperature sensitive (TS) in cells from patients with NALD and IRD but far less so in CG8 patients with the ZS phenotype.

Material and Methods

Cell Culture and DNA Transfection

Several skin fibroblast cell lines from CG8 patients with PBDs—including ZS GM07371, IRD GM08771, and NALD GM11335—were obtained from the Coriell Institute for Medical Research. Fibroblasts from Japanese CG-A (CG8) patients with ZS (A-02 and A-06) were from Gifu University (Imamura et al. 1998*b*); those from patients GM16865, GM16866, and PDL35167 were from the Kennedy-Krieger Institute. Fibroblasts from an unaffected control individual and CG8 patients with PBD were cultured at 37°C or 30°C in Dulbecco's modified Eagle medium high glucose supplemented with 10% fetal calf serum (Shimozawa et al. 1992; Imamura et al. 1998*a;* Tamura et al. 2001). CHO cell mutant ZP167 of CG8 (Ghaedi et al. 1999) was cultured at 37°C or 30°C, as described elsewhere (Tamura et al. 2001). DNA transfection to CHO cells and patient fibroblasts was respectively performed by using Lipofectamine (Life Technologies) and by electroporation using a Gene Pulser II electroporator (Bio-Rad) on setting at 320 V and 500 μF, as described elsewhere (Tamura et al. 1998). Human *PEX26* cDNA (GenBank accession number AB089678) was cloned by a functional complementation assay using CHO cell mutant ZP167 and a human kidney cDNA library constructed in pCMVSPORT (Tamura et al. 1998; Matsumoto et al. 2003).

Morphological Analysis

Peroxisomes in human fibroblasts and CHO cells were visualized by indirect immunofluorescence light microscopy, as described elsewhere (Shimozawa et al. 1992). We used rabbit antibodies to each of the following: human catalase (Matsumoto et al. 2001), PTS1 peptide (Otera et al. 1998), thiolase (Tsukamoto et al. 1990), and Pex14p C-terminal peptide (Shimizu et al. 1999). Antigen-antibody complexes were detected under a Carl Zeiss Axioskop FL microscope, using fluorescein isothiocyanate–labeled goat anti-rabbit immunoglobulin G (IgG) antibody (Cappel) or Texas Red–labeled goat anti-rabbit IgG antibody (Leinco Technologies). A stable transformant, named "ZP167EG2," of ZP167 cells expressing PTS2-tagged enhanced green fluorescent protein (PTS2-EGFP) was isolated, essentially as described by Yanago et al. (2002). PTS2 import was verified by monitoring the EGFP localization.

Mutation Analysis

Poly(A)$^+$ RNA was obtained from patient fibroblasts by using a QuickPrep mRNA purification kit (Amersham Biosciences). RT-PCR using poly(A)$^+$ RNA was conducted with a pair of human *PEX26*-specific PCR forward and reverse primers—1F (nucleotide sequence at 4–21) and 1R (nucleotide sequence at 915–898) or -1F (nucleotide sequence at −20 to −1) and 1R (table 1)—to cover a full-length *PEX26* ORF. Nucleotide sequence of the PCR products cloned into pGEM.T easy vector (Promega) was determined by the dideoxy-chain termination method using a Dye-terminator DNA sequence kit (Applied Biosystems). Patient-derived *PEX26* cDNAs—in-

Table 1

Synthetic Oligonucleotide Primers Used

Primer[a]	Sequence[b] (5′→3′)
1F	AAGCTTGAGATCTCTAAGAGCGATTCTTCGACC [4–21]
-1F	GCCTTGGACCCGGACTCGTT [−20 to −1]
1R	CAGGGAAGATCTGTCACGGATGCGGAGCTG [915–898]
2F	AAGTCCTGGAGCTGTGCA [356–373]
-2F	ACAGAAGGCGATGGGCCGAG [−206 to −187]
2R	GCTGGATCAAATCTCACC [815–798]
3R	CACAGCTCCAGGCTCTTG [411–394]
97F	CTGGAGATCTCTGATCGGTGGCAAGAAGTC
Not.R	GCCCGCGGCCGCTCAGTCACGGATGCGGAG [915–901 plus stop codon]
g1F	TTCTGCTGACAGCTCATTGG
g1R	ACTTACCACAGCTCCAGGAC
g3F	GCGGTCACTCCGACGTCTGAGGACCTGGGC
g3R	GCCCGGAAATCGGTTCATTTCCGAGCCCAG
T35insCF	CTGCAGCCCCCCCTCAGGGGGCTCGGGG
T35insCR	CCCTGAGGGGGGGCTGCAGAGGTCGAAG
e1F	AACTCGGGATATCCCGGAGCCTCTGGGGAG
e1R	TGGGAAGGACAGAACTCCTGAGACCTTGAG
SP6	ATTTAGGTGACACTATAG

[a] F = forward primer; R = reverse primer.
[b] Positions of the underlined nucleotide sequences are given in brackets.

cluding *PEX26G89R, PEX26R98W, PEX26L45P,* and *PEX26G255insT*—were cloned into pCMVSPORT I vector by replacing the *Bss*HII-*Pma*CI fragment (nucleotide sequence at 75–487) of *PEX26* from a control individual with that of the respective patient's *PEX26* in pGEM.T easy. *PEX26M1T* was constructed as follows: PCR was done using as template the RT product from GM08771 RNA and primers -2F and 3R; the *Eco*RV-*Bss*HII fragment was inserted into *Eco*RV-*Bss*HII sites of pCMVSPORT•*PEX26*. pCMVSPORT•*PEX26T35insC* was generated by two-step PCR: the first PCR was done with sets of SP6 and T35insC.R, and T35insC.F and 3R; the second PCR was done with SP6 and 3R. Its *Sal*I-*Bss*HII fragment was cloned into the *Sal*I-*Bss*HII site of pCMVSPORT•*PEX26*. pCMVSPORT•*PEX26T35insC/del223-271* was constructed by replacing the *Pma*CI-*Bam*HI fragment of pCMVSPORT•*PEX26T35insC* with that of *PEX26del223-271* in pGEM.T. Transfection was done to fibroblasts by electroporation and to ZP167 by lipofection. Genomic DNA was prepared from cultured fibroblasts, as described elsewhere (Honsho et al. 1998). To investigate the zygosity of a *PEX26* mutant allele, we performed PCR amplification using a pair of forward and reverse primers: g1F and g1R for the nucleotide residues at 231–371 in the *PEX26* ORF and g3F and g3R for the nucleotide residues at 1–230 of *PEX26* ORF (table 1). PCR products were directly sequenced.

Generation of Mutant Constructs

An epitope Flag-tagging to the N-terminus of Pex26p was done as follows. The full-length *PEX26* was amplified using a pair of primers: 1F and Not.R for nucleotide sequence at 915–901. The PCR product was digested with *Bgl*II and *Not*I and was then ligated into the *Bam*HI-*Not*I sites of pCMVSPORT•*Flag-PEX1* (Tamura et al. 2001). A *Flag-PEX26* mutant, *Flag-PEX26T35insC,* was likewise constructed from PCR product by using primers 1F and Not.R and, as a template, pCMVSPORT•*PEX26T35insC. Flag-PEX26M1T* was constructed as follows: PCR was done using primers 97F (designed for translation starting at the second Met, at position 97) and Not.R. The *Bgl*II-*Not*I fragment of PCR product was ligated into the *Bam*HI-*Not*I sites of pCMVSPORT•*Flag-PEX1. Flag*-tagged *PEX26* mutants in pCMVSPORT—*PEX26G89R, PEX26R98W, PEX26L45P,* and *PEX26G255insT*—were generated by replacing the *Bss*HII-*Pma*CI fragment (nucleotide sequence at 75–487) of *PEX26* from a control individual with the respective patient's *PEX26* in pGEM.T easy.

Other Methods

Western blot analysis was done using a set of primary rabbit antibodies and a second antibody, donkey anti-rabbit IgG antibody conjugated to horseradish peroxidase (Amersham Biosciences), or using mouse anti-Flag antibody (M2; Sigma) and horseradish peroxidase-labeled donkey anti-mouse IgG antibody (Amersham Biosciences). A multiple-tissue northern blot (Clontech) was probed with ^{32}P-labeled *PEX26* cDNA amplified with primers 2F and 2R and full-length β-actin cDNA (Clontech). Washing was done twice with 0.1 × SSPE

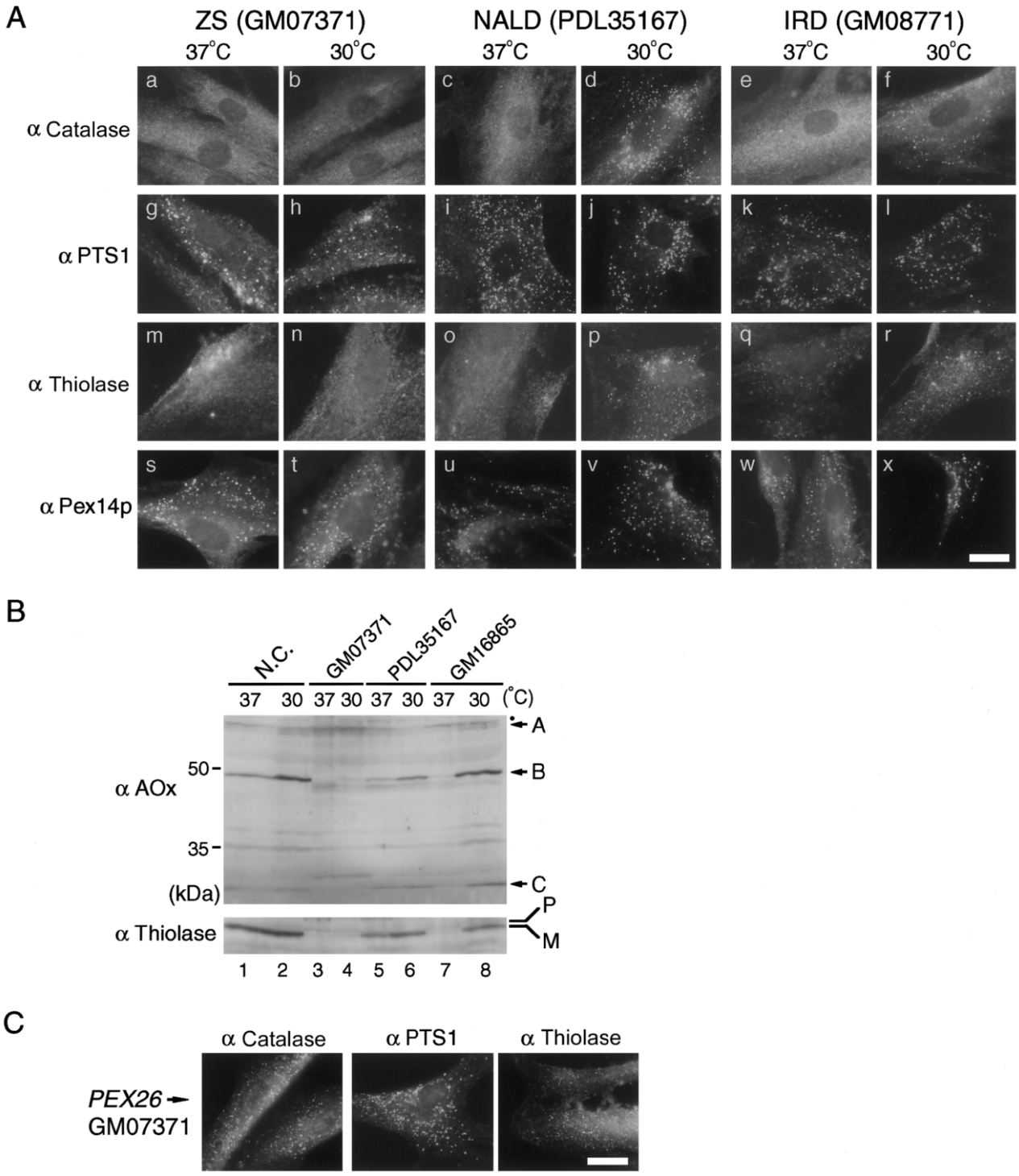

Figure 1 Phenotype of peroxisome deficiency in fibroblasts from CG8 patients. *A,* Patient-derived fibroblasts, cultured for 3 d at 37°C or 30°C and then stained with antibodies to catalase (*a–f*), PTS1 (*g–l*), a PTS2 protein (thiolase) (*m–r*), and Pex14p (*s–x*). Fibroblasts were derived from a patient with ZS (GM07371) (*left panels*), a patient with NALD (PDL35167) (*middle panels*), and a patient with IRD (GM08771) (*right panels*). Magnification 630×; bar = 30 μm. *B,* Biogenesis of peroxisomal proteins. Fibroblasts (~10^5 cells) from a normal control individual and from CG8 patients with PBDs were cultured for 3 d at 37°C or 30°C. Cell lysates were subjected to SDS-PAGE and were transferred to a polyvinylidene difluoride membrane. Immunoblot analysis was done using rabbit antibodies to AOx (*upper panel*) and thiolase (*lower panel*). *Lanes 1* and *2,* Normal control (N.C.). *Lanes 3* and *4,* Patient with ZS (GM07371). *Lanes 5* and *6,* Patient with NALD (PDL35167). *Lanes 7* and *8,* Patient with IRD (GM16865). Molecular markers are at left. "A," "B," and "C" denote 75-, 53-, and 22-kDa AOx components, respectively. The dot (•) shows a nonspecific band (Tamura et al. 2001). "P" and "M" denote a larger precursor protein and a mature protein of thiolase, respectively. *C, PEX26* expression, restoring the impaired protein import to peroxisomes in PBD fibroblasts. GM07371 fibroblasts were transfected with *PEX26* and were stained as in panel A, 3 d after the transfection. Bar = 30 μm.

Table 2

Phenotypes and Genotypes of Fibroblasts from CG8 Patients with PBDs

Patient (Sex)	Age at Death or Last Follow-Up	TS[a] of (%)						Mutation(s)	
		Catalase		PTS1		Thiolase (PTS2)			
		37°C	30°C	37°C	30°C	37°C	30°C	RT-PCR [Clones][b] (nt→aa)	Genomic PCR
ZS GM07371 (F)	3 wk	0	0	80	90	0	0	T35insC→fs/ter [12/12] T35insC/del223-271 [6/12]	T35insC/T35insC …[c]
ZS A-02 (M)	11 mo	0	15	100	100	0	10	G265A→G89R [12/12]	G265A/G265A
ZS A-06 (F)	4 mo	0	15	100	100	0	5	G265A→G89R [12/12]	G265A/G265A
ZS GM16866[d]	14 wk gestation	0	5	80	90	0	20	…[e]	…[e]
NALD GM11335 (F)	6 years	15	65	100	100	30	70	C292T→R98W[f] [10/10]	C292T/C292T
NALD PDL35167 (M)	10 years	5	50	100	100	50	90	C292T→R98W [11/11]	C292T/C292T
IRD GM08771 (F)	4 years	10	40	100	100	60	90	T2C→M1T [3/12] T134C→L45P [9/12]	T2C/T2 T134C/T134
IRD GM16865 (F)	12 years	15	70	100	100	30	80	C292T→R98W [10/16] G255insT→fs/ter [6/16]	C292T/C292 G255insT/G255
Control		100	100	100	100	100	100		

[a] The percentage of peroxisome-positive cells was the mean of total cell number counted in two separate areas under a microscope, where the range was ~10% of respective mean values.
[b] nt = Nucleotide; aa = amino acid; fs/ter = frameshift resulting in termination.
[c] Not determined.
[d] Sex of fetus not checked.
[e] No RT-PCR products were obtained.
[f] Matsumoto et al. 2003.

(15 mM NaCl, 0.865 mM NaH_2PO_4, and 0.125 mM EDTA)/0.1% SDS at 55°C.

Results

Normal Import of PTS1—and TS Catalase and PTS2 Import in CG8 Fibroblasts

Catalase was detected in a diffuse staining pattern, indicative of cytosolic localization, in fibroblasts derived from a CG8 patient with ZS (GM07371) at 37°C (fig. 1*A* [*a*]), whereas cells of several patients, including NALD PDL35167 and IRD GM08771, were positive but with many fewer catalase-containing particles (fig. 1*A* [*c* and *e*]) than in normal cells (data not shown). Catalase was likewise localized in the cytosol in fibroblasts from the other three CG8 patients with ZS (table 2). When cultured for 3 d at 30°C, fibroblasts from all of the patients with NALD and IRD were morphologically restored for catalase import or showed the increase in number of catalase-positive particles (fig. 1*A* [*d* and *f*]), indicative of the morphological TS phenotype. In ZS-type fibroblasts, at 30°C, catalase was not imported (e.g., in fibroblasts from patient GM07371; see fig. 1*A* [*b*]) or was restored only slightly (e.g., in fibroblasts from patient A-02; see table 2). In contrast, PTS1 proteins were observed in numerous punctate structures in fibroblasts derived from all of the patients with the three types of CG8 PBDs examined, at both temperatures (fig. 1*A* [*g–l*]), suggesting normal import of PTS1 proteins into peroxisomes. In ZS fibroblasts, thiolase, a PTS2 protein, was detected in a cytosolic staining pattern, indicating that PTS2 import was affected (fig. 1*A* [*m*]). In fibroblasts from two patients with IRD (GM08771 and GM16865) and a patient with NALD (PDL35167), thiolase was discernible in a punctate staining pattern, indicative of normal but less efficient PTS2 import (fig. 1*A* [*o* and *q*] and table 2). By shifting to 30°C, we increased thiolase-positive peroxisomes in number in PTS2-positive cells from patients with NALD and IRD (fig. 1*A* [*p* and *r*] and table 2). Pex14p-positive particles were seen at both temperatures in all of the CG8 PBD fibroblasts (fig. 1*A* [*s–x*]), indicative of normal import of peroxisomal membrane proteins. In fibroblasts from an unaffected control individual, numerous peroxisomes were present at both temperatures (table 2).

In mammals, AOx is synthesized as a 75-kDa polypeptide, named the "A" component, and is proteolytically converted into 53-kDa "B" and 22-kDa "C" polypeptide components in peroxisomes (Miyazawa et al. 1989; Shimozawa et al. 1992). AOx components (A–C) were evident in normal fibroblasts cultured at 37°C, as well as at 30°C (fig. 1*B*, *upper panel* [*lanes 1* and *2*]). AOx-A–C components were likewise detectable in fibroblasts from patients with PBDs (namely, NALD PDL35167 and IRD GM16865) at 37°C and more strongly at 30°C (fig. 1*B* [*lanes 5–8*]), at which temperature PTS1 and PTS2 pro-

Table 3

CGs of Patients with PBDs and *PEX* Genes

U.S./European (Japanese) CG Designation	Phenotype(s)[a]	Gene
CG8 (CG-A)	ZS, NALD,[b,c] IRD[b,c]	*PEX26*
CG1 (CG-E)	ZS, NALD, IRD[c,d,e]	*PEX1*
CG2	ZS, NALD	*PEX5*
CG3	ZS, NALD, IRD	*PEX12*
CG4[f] (CG-C)	ZS, NALD[c]	*PEX6*
CG7[g] (CG-B)	ZS, NALD	*PEX10*
CG9 (CG-D)	ZS	*PEX16*
CG10 (CG-F)	ZS, IRD[c]	*PEX2*
CG11 (CG-R)	RCDP	*PEX7*
CG12 (CG-G)	ZS	*PEX3*
CG13 (CG-H)	ZS, NALD[h]	*PEX13*
CG14 (CG-J)	ZS	*PEX19*

[a] Cell phenotypes showing reported TS protein import to peroxisomes are also indicated.
[b] Present study.
[c] Imamura et al. 1998*b*.
[d] Imamura et al. 1998*a*.
[e] Walter et al. 2001.
[f] Including former CG6.
[g] Including former CG5.
[h] Shimozawa et al. 1999.

teins were mostly in punctate structures, which were peroxisomes (see fig. 1*A* [*i–l* and *o–r*] and table 2). In contrast, in fibroblasts from patient ZS GM07371, conversion of AOx-A to AOx-B and -C components was undetectable at 37°C but became barely discernible at 30°C, whereas PTS1 proteins were in punctate structures at both temperatures, presumably in peroxisomal-remnant–like particles (see fig. 1*A* [*g* and *h*]). A protease required for AOx conversion may not be imported or may be much less functional in these cells. Peroxisomal thiolase is synthesized as a larger, 44-kDa precursor with an amino-terminal cleavable PTS2 and is processed to its mature size, 41 kDa, in peroxisomes (Tsukamoto et al. 1990; Shimozawa et al. 1992; Mukai et al. 2002). In normal fibroblasts, only the mature thiolase was detected at both temperatures (fig. 1*B, lower panel* [*lanes 1* and *2*]), thereby demonstrating rapid processing of the precursor form. The mature form was likewise detectable at both temperatures in NALD PDL35167 cells (fig. 1*B, lower panel* [*lanes 5* and *6*]), in which most of the thiolase was apparently imported (see fig. 1*A* [*o* and *p*] and table 2). In contrast, only the larger precursor was found at 37°C in ZS GM07371 fibroblasts (fig. 1*B, lower panel* [*lane 3*]), implying a defect of thiolase import and processing activity. Only partial processing was noted at 30°C (fig. 1*B, lower panel* [*lane 4*]). The thiolase precursor was mostly processed to the mature form at 30°C in IRD GM16865 fibroblasts (fig. 1*B, lower panel* [*lane 8*]), whereas both forms of thiolase were detectable at 37°C, but only at a very low level (fig. 1*B, lower panel* [*lane 7*]). The extent of thiolase processing thus is apparently consistent with the morphological TS phenotype of thiolase import (see fig. 1*A* [*m–r*] and table 2).

Fibroblasts from patient ZS GM07371 were morphologically complemented for peroxisome assembly at 37°C by transfection of *PEX26* (fig. 1*C*). The import of peroxisomal proteins was likewise restored in fibroblasts derived from CG8 patients with PBDs, including those from patients NALD PDL35167 and IRD GM16865 (data not shown). These results indicate that dysfunction of *PEX26* is responsible for the impaired biogenesis of peroxisomes in CG8 patients (table 3).

Identification of Mouse PEX26

By a homology search of the mouse DNA database, using "human *PEX26*" as a search term, we identified a potential mouse homologue (GenBank accession number AK014598). Mouse and human *PEX26* proteins were identical in amino acid length, with 74% identity at an amino acid level, despite demonstration that a 4-amino-acid deletion was mutually aligned at two different places (fig. 2*A*).

Mutation Analysis of CG8 Patients

Patients with ZS: T35insC.—To characterize the dysfunction of *PEX26* in CG8 patients with ZS, we isolated *PEX26* cDNA from fibroblasts from a patient (GM07371) and an unaffected control individual by means of RT-PCR. Subsequent sequencing of cDNA clones from the patient indicated a point mutation resulting in a 1-base (C) insertion at nucleotide position T35 (with the A of the initiating ATG being 1), in a codon (CTC) for Leu[12], resulting in a frameshift in-

Figure 2 (p. 239) Mutation analysis of *PEX26* in CG8 patients with PBDs. *A,* Deduced amino acid sequence alignment of human (*Hs*) and mouse (*Mm*) Pex26p. For human and mouse *PEX26* cDNAs, see GenBank (accession numbers AB089678 and AK014598, respectively). Dashes (–) represent spaces. A membrane-spanning segment is indicated by a line above it. *B,* Mutation analysis by PCR. *Left,* Nucleotide sequence of *PEX26* from CG8 patients with PBDs, determined by RT-PCR. Partial sequence and deduced amino acid sequence of *PEX26* cDNAs from a normal control and patients with ZS (GM07371 and A-02) and IRD (GM08771 and GM16865) are shown. RT-PCR products from GM16865 also showed the R98W mutation (see table 2). *Right,* PCR for control DNA and patient-derived fibroblasts. Nucleotide sequence of PCR products was determined. The nucleotide sequence for DNA from patients (A-02 and GM16865) was determined for the sense strand (*above*). Mutations identified were deposited in GenBank: T35insC (accession number AB103104), T35insC/del223-271 (accession number AB103105), G89R (accession number AB103106), R98W (accession number AB103107) (Matsumoto et al. 2003), M1T (accession number AB103108), L45P (accession number AB103109), and G255insT (accession number AB103110).

A

```
HsPex26p   1 MKSDSSTSAAPLRGLGGPLRSSEPVRAVPARAPAVDLLEEAADLLVVHLDFRAALETCERAW 62
MmPex26p   1 MKSDASTSAAPLKGLVGPLRSSEPALALPAVSPAVHLLEEASDLLVVHLDFHAALETCERAW 62

HsPex26p  63 QSLANHAVAEEPAGTSLEVKCSLCVVGIQALAEMDRWQEVLSWVLQYYQVPEKLPPKVLELC 124
MmPex26p  63 QSLA----EEPVSGTIVEVKCSLCVVGIQALAEMDRWREALSWVLRYYQVPEKLPPKVLELC 120

HsPex26p 125 ILLYSKMQEPGAVLDVVGAWLQDPANQNLPEYGALAEFHVQRVLLPLGCLSEAEELVVGSAA 186
MmPex26p 121 ILLYSKMKEPGAVLDVASAWLQDPDNQGLPDYGSLARLHVFRLLLPSGRLSEAEELAVRSAA 182

HsPex26p 187 FGEERRLDVLQAIHTARQQQ----KQEHSGSEEAQKPNLEGSVSHKFLSLPMLVRQLWDSAV 244
MmPex26p 183 FSEEQRVEALQAIHLARQQHTQEHTQEHSDSQEPQKLRQEGSFSQKLLSLLMLLRRLWGSVV 244

HsPex26p 245 SHFFSLPFKKSLLAALILCLLVVRFDPASPSSLHFLYKLAQLFRWIRKAAFSRLYQLRIRD 305
MmPex26p 245 SHLLSQPFRKGLLAALILCLLILRFDPAAPSSLPFLYQLTQLFRRIQKATLSRLYPLALRD 305
```

B

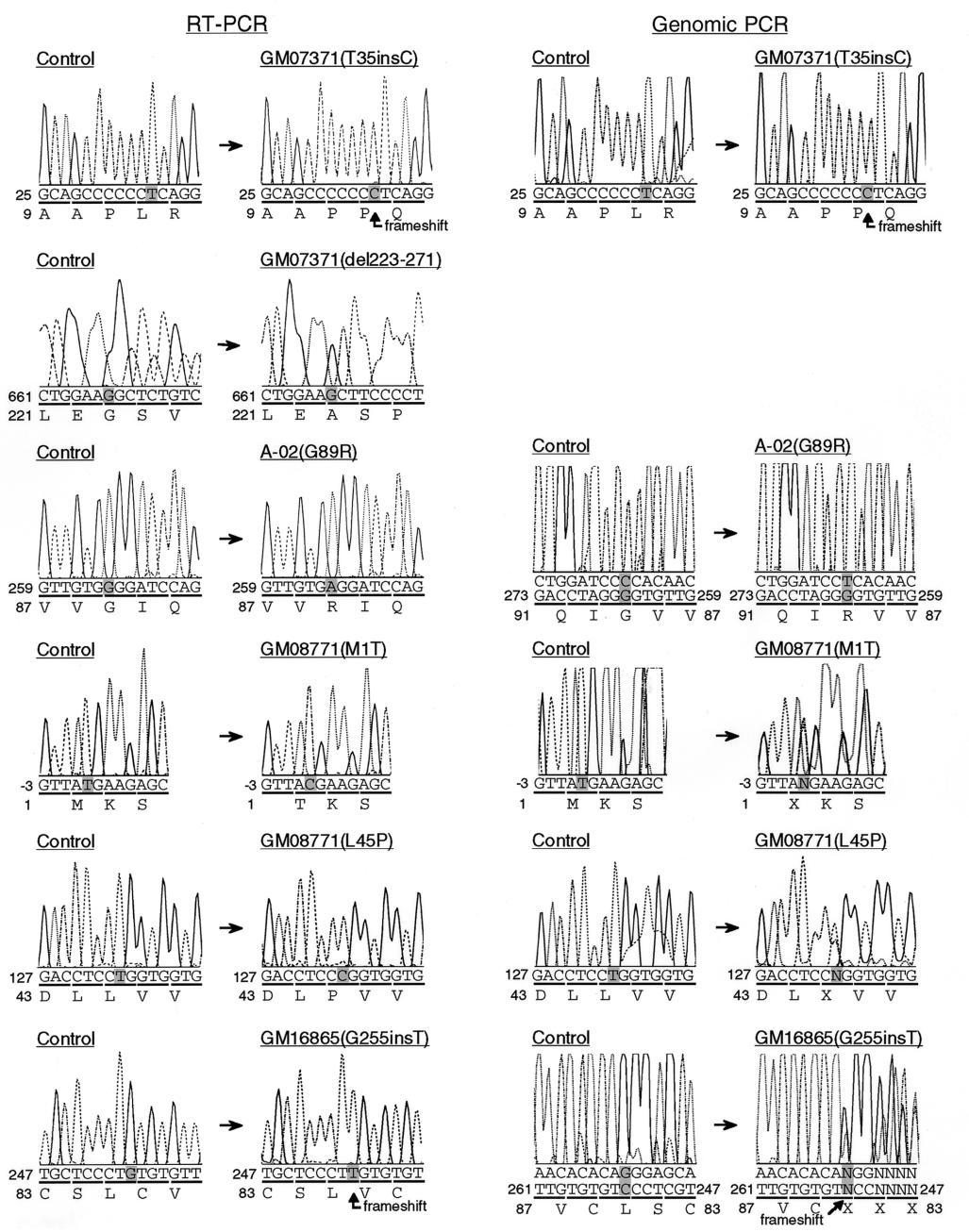

ducing a 102-amino-acid sequence distinct from normal Pex26p (fig. 2*B, left panel*). Of 12 cDNA clones isolated, all showed the same site mutation, termed "*PEX26T35insC,*" thereby suggesting a homozygous mutation. Furthermore, six clones showed an additional mutation: deletion of nucleotide residues at 668–814, encoding amino acid residues at 223–271 (fig. 2*B, left panel*).

To determine the zygosity of a mutant allele, we performed genomic PCR to amplify the sequence corresponding to nucleotide residues 1–230 in the *PEX26* ORF. Only a single type of nucleotide sequence giving rise to the T35insC mutation was identified in the PCR products (fig. 2*B, right panel*). A *PEX26* mutation resulting in the deletion of amino acid residues at 223–271 was not defined. Taken together, these findings—namely, T35insC and T35insC plus a mutation responsible for deletion of 223–271—make it likely that this patient with ZS was a compound heterozygote. *PEX26T35insC* was functional in catalase import (figs. 3*A* and 3*B* [*a* and *h*]), as well as in transport of PTS1 and PTS2 proteins (table 4), which resulted in formation of peroxisomes, as assessed by transfection to a *pex26* ZP167 mutant and ZP167EG2 cells expressing PTS2-EGFP. Expression of *PEX26T35insC/del223-271* in ZP167 gave restoration of peroxisomes very weakly at 37°C and more efficiently at 30°C (fig. 3*B* [*b* and *i*] and table 4). Cotransfection of *PEX26T35insC* and *PEX26T35insC/del223-271* to ZP167 showed a phenotype similar to GM07371 fibroblasts, only in PTS1 import (table 4). Weak catalase import and positive PTS2 import may be due to a higher level of expression of these two types of Pex26p mutants.

Patients with ZS: G89R.—RT-PCR was likewise done using poly(A)$^+$ RNA from another CG8 patient with ZS (A-02; Gifu University). Sequencing of cDNA clones showed a point mutation of nucleotide G to A at position 265 in a codon (GGG) for Gly^{89}, resulting in a codon (AGG) for Arg (fig. 2*B, left panel*). Of 12 cDNA clones isolated, all showed the same mutation, termed "*PEX26G89R,*" thereby suggesting a homozygous mutation. Exactly the same mutation at nucleotide substitution G265A, resulting in missense G89R mutation, was identified in the RT-PCR products from fibroblasts from an unrelated patient with ZS (A-06) (table 2). To determine the zygosity of a *PEX26G89R* mutant allele in these two patients with ZS, we performed genomic PCR to amplify the sequence corresponding to nucleotide residues 231–371 in the *PEX26* ORF. Only a single type of nucleotide sequence with G265A was identified in the PCR products from both patients (fig. 2*B, right panel,* and table 2), indicating that the patients with ZS (A-02 and A-06) were homozygous for the G89R mutation. This mutation inactivated the function of *PEX26,* as assessed by transfection of *PEX26G89R* to CHO cell mutant ZP167, which resulted in the phenotype of deficiency with weak TS import of catalase and PTS2-EGFP (figs. 3*B* [*c* and *j*] and 3*C, left panel* [*b* and *d*], and table 4) and in TS-dependent PTS1 import that was competent but less potent (fig. 3*C, left panel* [*a* and *c*], and table 4), similar to that of the patient-derived fibroblasts. Biogenesis of peroxisomal proteins, AOx and thiolase, was verified in *PEX26G89R*-transfected ZP167 cells. Conversion of AOx-A to AOx-B and -C components and processing of thiolase were detected only in cells cultured at 30°C (fig. 3*D* [*lanes 3* and *4*]), reproducing a TS phenotype as noted in morphology in ZP167 expressing Pex26pG89R (and patient fibroblasts), whereas ZP167 transfected with normal *PEX26* showed such proteolytic changes at both temperatures (fig. 3*D* [*lanes 1* and *2*]). These findings imply the importance of the N-terminal part encompassing Arg^{89} of Pex26p in its biological activity. It is plausible that the G→R missense mutation may affect the configuration of Pex26p.

From poly(A)$^+$ RNA from another CG8 patient with ZS (GM16866), no detectable RT-PCR product was obtained (table 2), indicating that *PEX26* mRNA was under the detection level. *PEX26* may be defective at the level of transcription, or it may be expressed but unstable and degraded.

Patients with NALD: R98W.—To determine the dysfunction of *PEX26* in a CG8 patient with NALD (PDL35167), we cloned and sequenced RT-PCR products. Of 11 cDNA clones isolated, all showed a point mutation of nucleotide C to T at position 292 in a

Figure 3 (p. 241) Transformation of a CHO *pex26* mutant (ZP167) with patient's *PEX26. A,* Schematic representation of Pex26p and mutation sites in patients with PBDs. "TM" designates a membrane-spanning segment. *B, PEX26* cDNAs derived from CG8 patients with PBDs, transfected to ZP167. Transfection was done with ZS GM07371–derived *PEX26T35insC* (*a* and *h*) and *PEX26T35insC/del223-271* (*b* and *i*), ZS A-02–derived *PEX26G89R* (*c* and *j*), NALD PDL35167–derived *PEX26R98W*(*d* and *k*), IRD GM08771–derived *PEX26M1T* (*e* and *l*) and *PEX26L45P* (*f* and *m*), and IRD GM16865–derived *PEX26G255insT* (*g* and *n*). Cells were cultured for 3 d at 37°C (panels *a–g*) or 30°C (*h–n*) and were stained with anti-catalase antibody. Magnification 630×; bar = 20 μm. *C,* ZP167EG2 cells expressing PTS2-EGFP, likewise transfected with *PEX26G89R* (*left*) and *PEX26R98W* (*right*). Import of proteins with PTS1 and PTS2 was verified by cell staining with anti-PTS1 antibody and by monitoring of PTS2-EGFP. Bar = 20 μm. *D,* Biogenesis of AOx and thiolase. Cell lysates (~10^4 cells) of *PEX26G89R*- or *PEX26R98W*-transfected ZP167 that had been cultured for 3 d at 37°C (*lanes 1, 3,* and *5*) or 30°C (*lanes 2, 4,* and *6*) were analyzed by immunoblot, using antibodies to AOx (*left*) and thiolase (*right*). Molecular markers are given at left. "A"–"C" denote AOx components. Dots (•) show nonspecific bands. "P" and "M" denote a larger precursor protein and a mature protein of thiolase, respectively.

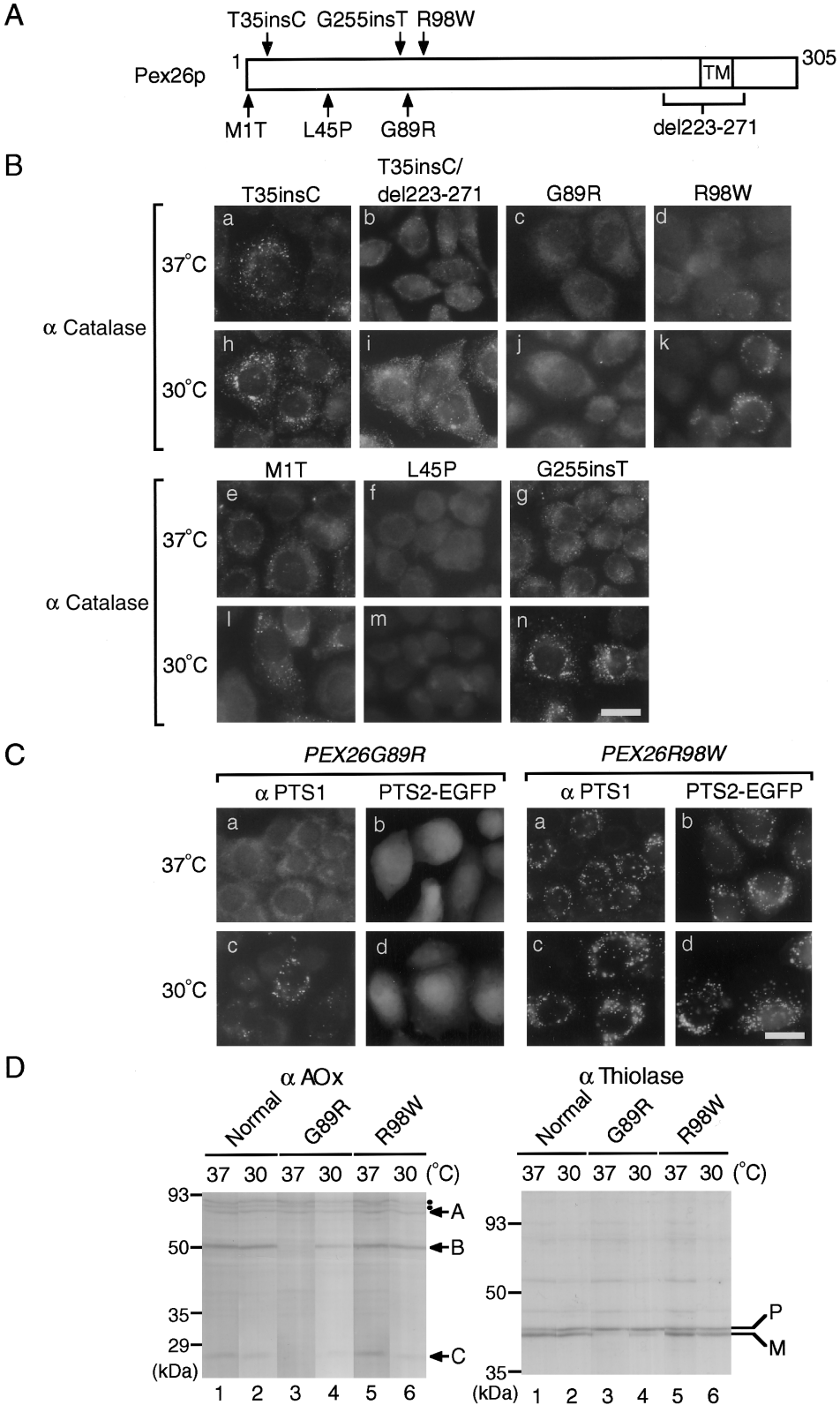
A
T35insC G255insT R98W
Pex26p
1
305
TM
M1T L45P G89R
del223-271
B
T35insC
T35insC/
del223-271
G89R
R98W
α Catalase
37°C
30°C
M1T
L45P
G255insT
C
PEX26G89R
PEX26R98W
α PTS1
PTS2-EGFP
D
α AOx
α Thiolase
Normal
G89R
R98W
37 30 37 30 37 30 (°C)
93
50
35
29
(kDa)
A
B
C
P
M
1 2 3 4 5 6

Table 4

Transfection of Patient-Derived *PEX26* to CHO *pex26* Mutant ZP167

	TS[a] OF (%)					
	Catalase		PTS1		PTS2-EGFP[b]	
PEX26 MUTANT	37°C	30°C	37°C	30°C	37°C	30°C
Wild type[c]	100	100	100	100	100	100
T35insC	70	90	90	90	90	90
T35insC/del223-271	5	10	5	45	5	20
G89R	0	5	5	55	0	10
R98W	5	70	65	85	100	100
M1T	55	70	60	95	60	80
L45P	0	0	0	5	0	0
G255insT	0	40	70	90	75	75
Coexpression:						
T35insC + T35insC/del223-271	5	20	85	80	80	80
M1T + L45P	50	70	55	90	100	100
R98W + G255insT	0	60	70	85	90	90

[a] The percentage of peroxisome-positive cells was the mean of total cell number counted in two separate areas under a microscope, where the range was ~10% of respective mean values.

[b] PTS2 import was assessed with PTS2-tagged EGFP.

[c] Of the cells, 60%–80% complemented by *PEX26* transfection; import-restoring activity of *PEX26* mutants was represented as a percentage of normal Pex26p.

codon (CGG) for Arg^{98}, resulting in a codon (TGG) for Trp, termed "*PEX26R98W*" (data not shown), strongly suggesting that the patient is homozygous for the *PEX26R98W* allele, which is the same missense mutation recently identified in another patient with NALD (GM11335) (Matsumoto et al. 2003) (table 2). PCR and sequence analysis of the PDL35167 genomic sequence, encompassing nucleotide residues 231–371 in the *PEX26* ORF, showed one type of nucleotide substitution, C292T (table 2), indicating that this patient with NALD was homozygous for the mutation as identified for GM11335 (Matsumoto et al. 2003).

Expression of *PEX26R98W* in *pex26* ZP167 resulted in a morphological phenotype similar to that seen in the patient's fibroblasts in regard to import of catalase and PTS1 and PTS2 proteins (figs. 3*B* [*d* and *k*] and 3*C, right panel,* and table 4), confirming that *PEX26R98W* is the cause of NALD in these patients with PBDs. Biogenesis of AOx and thiolase in *PEX26R98W*-transfected ZP167 cells was similar to that in ZP167 expressing normal *PEX26,* showing that this is a milder form of the *PEX26* mutation (fig. 3*D* [*lanes 5* and *6*]).

Patients with IRD: M1T/L45P.—To delineate the dysfunction of *PEX26* in the CG8 patients with IRD, we sequenced *PEX26* cDNA cloned by RT-PCR from fibroblasts from a patient (GM08771), and we detected two types of point mutations: nucleotide T to C at position 2 in a codon (ATG) for the initiator Met^1 and at position 134 in a codon (CTG) for Leu^{45}, resulting in Thr^1 and Pro^{45}, respectively (fig. 2*B, left panel*). Of 12 cDNA clones isolated, 3 were with T2C, termed "*PEX26M1T,*" and 9 were with T134C, termed "*PEX26L45P,*" thereby suggesting a compound heterozygous mutation. To confirm the mutation sites and zygosity of mutant alleles, we performed genomic PCR at nucleotide residues 1–230 in the *PEX26* ORF. Two nucleotide substitutions were identified: one at position 2, T2C, together with normal T2; the other at T134C, with normal T134 (fig. 2*B, right panel*). We interpreted the results to mean that this patient with IRD (GM08771) was a compound heterozygote for the mutations.

PTS1-, catalase-, and PTS2-positive particles were discernible, in a mildly TS manner in the PTS1 and catalase import, in *PEX26M1T*-transfected ZP167 cells, whereas *PEX26L45P* expression did not restore the impaired peroxisome biogenesis in ZP167 (fig. 3*B* [*e, f, l,* and *m*] and table 4). An ~26-kDa protein band was detected using antibody to a Pex26p C-terminal peptide (data not shown), suggesting that Pex26pM1T was translated at the second Met, at position 96. In ZP167 cells that had been cotransfected with *PEX26M1T* and *PEX26L45P,* the morphological phenotype was similar to those of *PEX26M1T*-transfected cells and fibroblasts from patient GM08771, implying that *PEX26M1T* expression represents the phenotype of the patient-derived cells (table 4). It is less likely that Pex26pL45P affects on import of catalase and PTS1 and PTS2 proteins as a dominant-negative Pex26p.

Patients with IRD: R98W/G255insT.—In *PEX26* cDNA likewise isolated from fibroblasts from patient IRD GM16865, we identified a point mutation of nucleotide C to T at position 292, resulting in R98W, as in patients with NALD (table 2). Of 16 cDNA clones isolated, only 10 showed the same mutation, thereby

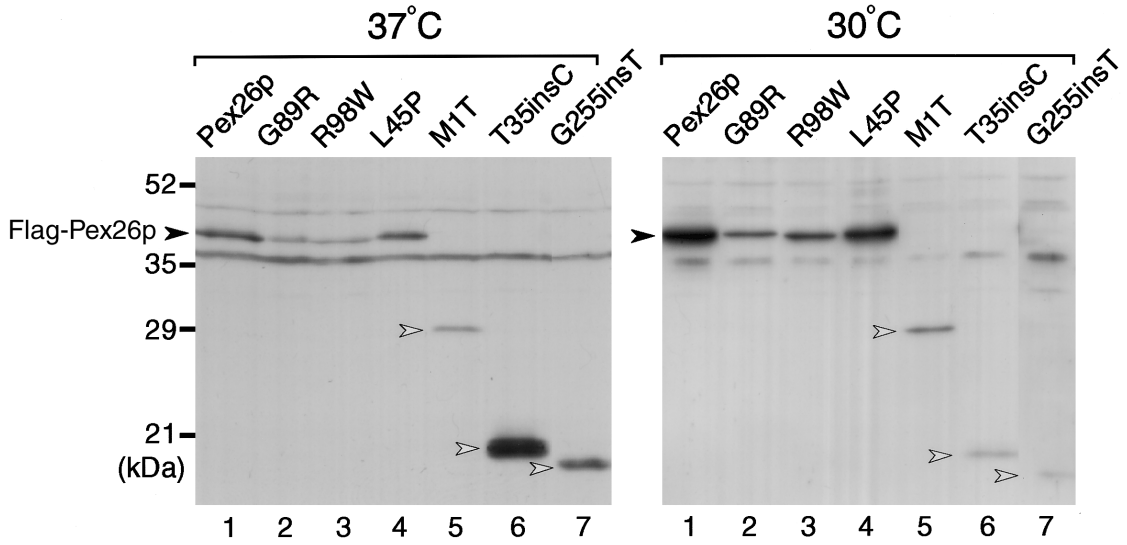

Figure 4 Expression level of Pex26p. ZP167 cells transfected with *Flag-PEX26* and its variants from CG8 patients were cultured for 3 d at 37°C (*left*) or 30°C (*right*). Cell lysates (~10^4 cells) were analyzed by SDS-PAGE and immunoblot, using anti-Flag antibody. Blackened arrowheads indicate the migration of Pex26p with authentic size; unblackened arrowheads indicate truncated forms of Pex26p.

suggesting a heterozygous mutation; the remaining 6 cDNA clones showed a point mutation resulting in a 1-base (T) insertion at nucleotide position 255 in a codon (CTG) for Leu[85], named "*PEX26G255insT,*" resulting in a frameshift inducing a 28-amino-acid sequence distinct from normal Pex26p (fig. 2*B, left panel*), in which the sequence at nucleotide position 292 was normal. These results indicate that patient GM16865 is a compound heterozygote. Zygosity of mutant alleles was assessed by genomic PCR at nucleotide residues 231–371 in the *PEX26* ORF. Two nucleotide substitutions were identified: C292T (not shown) and G255insT, both together with normal sequence (fig. 2*B, right panel*), confirming that this patient with IRD (GM16865) was a compound heterozygote for the mutations. *PEX26G255insT* expression in ZP167 resulted in TS-dependent catalase import (fig. 3*B* [*g* and *n*]), as well as PTS1- and PTS2-positive particles (table 4), similar to the phenotype of patient GM16865. Coexpression of *PEX26R98W* and *PEX26G255insT* also showed a similar morphology (table 4).

Collectively, these data demonstrate that the dysfunction of *PEX26* is responsible for peroxisome deficiency in CG8 PBDs.

Expressed Level of Mutated Pex26p

To investigate the expression level of Pex26p in normal cells and to determine to what extent the identified mutant forms of Pex26p are expressed in patient-derived cells, we performed western blotting of cell lysates, using antibodies against synthetic peptides comprising 17–19-amino-acid N- and C-terminal residues of Pex26p. No protein bands were detectable, even in normal cells, indicating that Pex26p is a very-low-abundance peroxin (data not shown). Therefore, we expressed the epitope Flag-tagged form of Pex26p and its variants in ZP167 cells. *Flag-PEX26T35insC* was expressed, resulting in a highly expressed distinct protein band with mass <20 kDa (fig. 4, *left panel* [*lane 6*]). Flag-Pex26pG89R was apparently much lower in the expressed level as compared with normal Flag-Pex26p (fig. 4, *left panel* [*lanes 1* and *2*]), suggesting that this mutant was unstable, presumably owing to degradation. Flag-Pex26pR98W was likewise detected in a lesser amount than Flag-Pex26pG89R (fig. 4, *left panel* [*lane 3*]), whereas Flag-Pex26pL45P was at a level similar to normal Flag-Pex26p (fig. 4, *left panel* [*lane 4*]). *Flag-PEX26M1T,* encoding Flag-Pex26p truncated from 1 to 96 (see the "Material and Methods" section), was likewise expressed in ZP167, in which the Pex26p variant was detected as a band with mass ~27 kDa, in a lesser amount than the normal type (fig. 4, *left panel* [*lane 5*]). This Pex26pM1T appears to be biologically active (see fig. 3*B* and table 4). Pex26pG255insT was normally expressed as an ~15-kDa protein (fig. 4, *left panel* [*lane 6*]). The results imply that mutations at Pex26pG89R and Pex26pR98W render Pex26p unstable and possibly partially degraded, thereby causing the impairment of peroxisome biogenesis in CG8 patients. Dysfunction of Pex26p variants, such as those with L45P, may arise from other effects, including an impaired interaction with other peroxins. The expressed level of

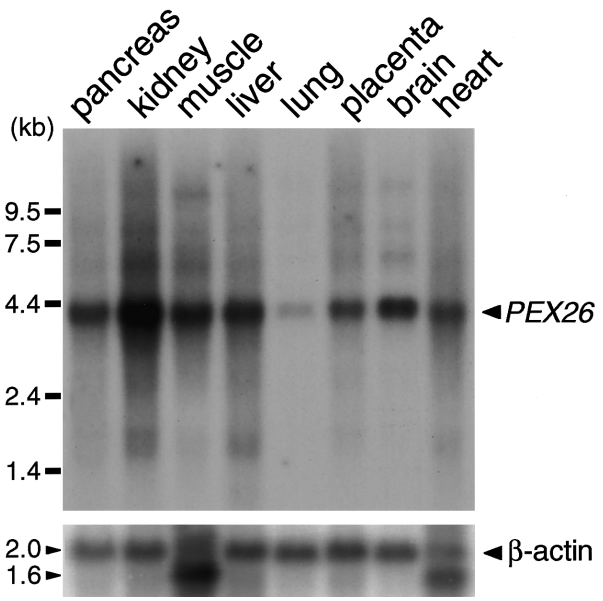

Figure 5 Expression of *PEX26* in human tissues. Northern blot analysis of poly(A)$^+$ RNA (2 μg) from pancreas, kidney, skeletal muscle, liver, lung, placenta, brain, and heart was done with a ^{32}P-labeled *PEX26* cDNA probe. RNA size markers are given at left. β-Actin cDNA was used to assess RNA load. An actin isoform RNA (1.6 kb) was also detected in muscle and heart. Exposure for *PEX26* was 3 d; exposure for β-actin was 16 h.

Pex26p variants, including normal Pex26p, was elevated at 30°C (fig. 4, *right panel*). The relation of the expressed Flag-Pex26p variants, such as those with T35insC and G255insT, to the morphological phenotype noted by expressing the untagged variants (fig. 3*B* and table 4) remains to be defined.

Tissue Expression of PEX26

The expression level of *PEX26* mRNA in different tissues was examined by northern blot analysis. A *PEX26* transcript with ~4.4 kb was detected as a major transcript in all of human tissues examined (fig. 5). The highest level of the *PEX26* transcripts was noted in kidney, and a relatively high level was detectable in liver, brain, and skeletal muscle. In several tissues, such as kidney and liver, a smaller transcript, with ~1.8 kb, was also detected. The *PEX26* expression pattern was similar to that of *PEX6,* except that the highest level of *PEX6* mRNA was in skeletal muscle (Yahraus et al. 1996), whereas *PEX5* and *PEX7* mRNAs showed distinct expression patterns (Dodt et al. 1995; Braverman et al. 1997).

Discussion

In the present study, we have demonstrated that impairment of *PEX26* is the genetic cause of CG8 PBDs. The genetic cause of CG8 PBDs had been sought for more than a decade. Expression of *PEX26* variants from CG8 patients in a *pex26* ZP167 nearly reproduced the phenotypes of the patient-derived fibroblasts, hence confirming that impaired *PEX26* is the genetic cause of CG8 disorders (table 4). Accordingly, *PEX26* is the 12th and last gene responsible for the PBDs of 12 CGs. The completion of the search for pathogenic genes responsible for 12 CGs of PBDs now makes it possible to conduct prenatal DNA diagnoses in all of the PBD CGs. CG8 is the third most common among the 11 PBDs and manifests clinically as ZS, NALD, and IRD (table 3) (Moser et al. 1995; Gould and Valle 2000). We investigated the cause of the variability of clinical manifestations in CG8 PBDs by analyzing the types and/or sites of mutations in *PEX26,* as well as the cell phenotype with respect to TS peroxisome biogenesis. Fibroblasts from all of the patients with ZS whom we examined showed defects in the import of catalase possessing a PTS1-like C-terminal KANL sequence and PTS2 thiolase, whereas import of PTS1 proteins was normal. Of the four patients with the ZS phenotype, a homozygous G89R mutation was identified in two patients, an undetectable level of *PEX26* mRNA was identified in the third patient, and a 1-base insertion at position 35 in one allele and the other allele with additional truncation was identified in the fourth patient. All of these mutations, as well as a mutation presumably resulting in a lack of detectable *PEX26* mRNA, appear to severely affect Pex26p in terms of functionally essential configuration and expression level, thus leading to the severe, ZS-type PBD. Only one type of mutation, R98W, was identified in two patients with NALD, giving rise to normal PTS1 import and less efficient import of catalase and PTS2 protein. Catalase and PTS2-protein import became more efficient in a TS manner. Similarly, in the two patients with IRD, we observed normal PTS1 import and TS-type import of catalase and thiolase. Thus, it is likely that *PEX26* mutations conferring the TS phenotype are the clinically milder NALD and IRD phenotypes, whereas those cells that are not TS lead to the severe ZS phenotype. Similar TS phenotypes were reported for patients of other CGs who have milder forms of PBDs (see table 3). It is noteworthy that the most common TS-type mutation in other peroxins was identified in Pex1p-defective patients with IRD who carry an allelic mutation in a codon for G843D (Imamura et al. 1998*a;* Tamura et al. 2001; Walter et al. 2001).

PEX26 mutations in the CG8 patients identified here are mostly located at the region encoding the N-terminal part of Pex26p, implying that this portion plays a crucial role in peroxisomal-protein import. Impaired function of these Pex26p variants was assessed by expression in *pex26* ZP167 cells. Pex26p with mutations (G89R and R98W) showed a phenotype similar to that seen in the patient-derived fibroblasts (table 4). Mis-

sense mutations of Pex26p, such as G89R and R98W, that apparently affect the configuration of Pex26p varied in respect to the TS phenotype; the TS R98W mutation was associated with the NALD phenotype, and the non-TS mutation was associated with the ZS phenotype. Coexpression of Pex26pM1T and Pex26pL45P reproduced the morphological phenotype observed in the patient-derived cells, as did *PEX26M1T*-transfected ZP167, in spite of complete loss of activity of Pex26pL45P; this implies that Pex26pL45P is not a dominant-negative mutant. Hence, given functionally active Pex26pM1T, it is more likely that translation started at the second, internally located methionine, at position 96—at least in the expression construct using a CMV promoter, the product of which migrated in SDS-PAGE at mass ~27 kDa. Likewise, coexpression of Pex26pR98W and Pex26pG255insT showed a phenotype similar to that in the patient-derived cells. Contrary to such a reproducible phenotype, coexpression of Pex26pT35insC and Pex26pT35insC/del223-271 failed to show the impaired import of catalase and PTS2, whereas Pex26pT35insC/del223-271 moderately represented the phenotype of the patient's morphology. This may be due to a different level of expression of each mutant Pex26p or translation at Met^{96} in transfection of *PEX26T35insC*. It is more likely that the T35insC mutation, creating Pex26p with normal sequence only up to amino acid at position 11, resulted in the most severely impaired phenotype, ZS. In addition, expression levels of Pex26p variants identified in CG8 patients were verified by the expression of Flag-tagged forms in ZP167 cells. Normal level of expression was noted in Pex26p with L45P, whereas a lower level was seen for Pex26p with G89R and R98W. From this viewpoint, it is conceivable that Pex26p variants with G89R and R98W reflect partly, if not completely, the phenotype noted in the patient-derived cells. A phenotype with missense mutations, G89R and R98W, as well as the T35insC mutation, creating Pex26p mutant with only normal 11-amino-acid plus distinct 102-amino-acid sequence, implies that the N-terminal part plays a role in the function of Pex26p in peroxisome biogenesis.

These findings raise several possibilities. Pex26p may play a direct role in the import of matrix proteins and may be required strictly for the import of catalase and PTS2 proteins but not for the import of PTS1 proteins. Alternatively, Pex26p may interact with a translocon involved in soluble-protein import, such as Pex14p, Pex13p, and RING peroxins (Fujiki 2000; Gould and Valle 2000; Otera et al. 2002). It is also possible that Pex26p may be involved in regulation of translocation steps of soluble peroxins, such as the PTS1 receptor Pex5p and the PTS2 receptor Pex7p, as well as Pex1p and Pex6p of the AAA ATPase family of peroxins (Fujiki 2000; Gould and Valle 2000). As a pivotal role of Pex26p, we very recently demonstrated that Pex26p functions in recruiting Pex1p-Pex6p complexes to peroxisome membranes (Matsumoto et al. 2003). Its underlying molecular mechanisms and dysfunctions remain to be defined.

Acknowledgments

We thank M. Obo, S. Okuno, and M. Okubo, for technical assistance; R. Tanaka, for preparing figures; and the other members of the Fujiki laboratory, for discussion. This work was supported, in part, by a SORST (Solution-Oriented Research for Science and Technology) grant (to Y.F.) from the Science and Technology Corporation of Japan; Grants-in-Aid for Scientific Research (12308033, 12557017, 12206069, 13206060, 14037253, 15032242, and 15207014 [all to Y.F.]), Grant of National Project on Protein Structural and Functional Analyses (to Y.F.), and the 21st Century COE Program, from the Ministry of Education, Culture, Sports, Science, and Technology of Japan; a grant from Uehara Memorial Foundation; a grant from Japan Foundation for Applied Enzymology; a grant (to S.T.) from Naito Foundation; and National Institutes of Health grant RR 00052 (to H.W.M.).

Electronic-Database Information

Accession numbers and the URL for data in this article are as follows:

GenBank, http://www.ncbi.nlm.nih.gov/Genbank/ (for human *PEX26* cDNA sequence [accession number AB089678]; *PEX26* with mutations T35insC [accession number AB103104], T35insC/del223-271 [accession number AB103105], G89R [accession number AB103106], R98W [accession number AB103107], M1T [accession number AB103108] L45P [accession number AB103109], and G255insT [accession number AB103110]; and mouse *PEX26* [AK014598])

Online Mendelian Inheritance in Man (OMIM), http://www.ncbi.nlm.nih.gov/Omim/ (for PBDs, ZS, NALD, IRD, and RCDP)

References

Braverman N, Steel G, Obie C, Moser A, Moser H, Gould SJ, Valle D (1997) Human *PEX7* encodes the peroxisomal PTS2 receptor and is responsible for rhizomelic chondrodysplasia punctata. Nat Genet 15:369–376

Dodt G, Braverman N, Wong CS, Moser A, Moser HW, Watkins P, Valle D, Gould SJ (1995) Mutations in the PTS1 receptor gene, *PXR1,* define complementation group 2 of the peroxisome biogenesis disorders. Nat Genet 9:115–125

Fujiki Y (2000) Peroxisome biogenesis and peroxisome biogenesis disorders. FEBS Lett 476:42–46

Ghaedi K, Honsho M, Shimozawa N, Suzuki Y, Kondo N, Fujiki Y (2000) *PEX3* is the causal gene responsible for peroxisome membrane assembly–defective Zellweger syndrome of complementation group G. Am J Hum Genet 67:976–981

Ghaedi K, Itagaki A, Toyama R, Tamura S, Matsumura T, Kawai A, Shimozawa N, Suzuki Y, Kondo N, Fujiki Y (1999) Newly identified Chinese hamster ovary cell mutants defective in peroxisome assembly represent complementation group A of human peroxisome biogenesis disorders and one novel group in mammals. Exp Cell Res 248:482–488

Gould SJ, Valle D (2000) Peroxisome biogenesis disorders: genetics and cell biology. Trends Genet 16:340–345

Honsho M, Tamura S, Shimozawa N, Suzuki Y, Kondo N, Fujiki Y (1998) Mutation in *PEX16* is causal in the peroxisome-deficient Zellweger syndrome of complementation group D. Am J Hum Genet 63:1622–1630

Imamura A, Tamura S, Shimozawa N, Suzuki Y, Zhang Z, Tsukamoto T, Orii T, Kondo N, Osumi T, Fujiki Y (1998*a*) Temperature-sensitive mutation in *PEX1* moderates the phenotypes of peroxisome deficiency disorders. Hum Mol Genet 7:2089–2094

Imamura A, Tsukamoto T, Shimozawa N, Suzuki Y, Zhang Z, Imanaka T, Fujiki Y, Orii, T, Kondo N, Osumi T (1998*b*) Temperature-sensitive phenotypes of peroxisome assembly processes represent the milder forms of human peroxisome-biogenesis disorders. Am J Hum Genet 62:1539–1543

Lazarow PB, Moser HW (1995) Disorders of peroxisome biogenesis. In: Scriver CR, Beaudet AI, Sly WS, Valle D (eds) The metabolic basis of inherited disease. Vol 7. McGraw-Hill, New York, pp 2287–2324

Matsumoto N, Tamura S, Fujiki Y (2003) The pathogenic peroxin Pex26p recruits the Pex1p–Pex6p AAA-ATPase complexes to peroxisomes. Nat Cell Biol 5:454–460

Matsumoto N, Tamura S, Moser A, Moser HW, Braverman N, Suzuki Y, Shimozawa N, Kondo N, Fujiki Y (2001) The peroxin Pex6p gene is impaired in peroxisome biogenesis disorders of complementation group 6. J Hum Genet 46: 273–277

Miyazawa S, Osumi T, Hashimoto T, Ohno K, Miura S, Fujiki Y (1989) Peroxisome targeting signal of rat liver acyl-coenzyme A oxidase resides at the carboxy terminus. Mol Cell Biol 9:83–91

Morand OH, Allen L-AH, Zoeller RA, Raetz CRH (1990) A rapid selection for animal cell mutants with defective peroxisomes. Biochim Biophys Acta 1034:132–141

Moser AB, Rasmussen M, Naidu S, Watkins PA, McGuiness M, Hajra AK, Chen G, Raymond G, Liu A, Gordon D, Garnaas K, Walton DS, Skjeldal OH, Guggenheim MA, Jackson LG, Elias ER, Moser HW (1995) Phenotype of patients with peroxisomal disorders subdivided into sixteen complementation groups. J Pediatr 127:13–22

Mukai S, Ghaedi K, Fujiki Y (2002) Intracellular localization, function, and dysfunction of the peroxisome-targeting signal type 2 receptor, Pex7p, in mammalian cells. J Biol Chem 277: 9548–9561

Otera H, Setoguchi K, Hamasaki M, Kumashiro T, Shimizu N, Fujiki Y (2002) Peroxisomal targeting signal receptor Pex5p interacts with cargoes and import machinery components in a spatiotemporally differentiated manner: conserved Pex5p WXXXF/Y motifs are critical for matrix protein import. Mol Cell Biol 22:1639–1655

Otera H, Tateishi K, Okumoto K, Ikoma Y, Matsuda E, Nishimura M, Tsukamoto T, Osumi T, Ohashi K, Higuchi O, Fujiki Y (1998) Peroxisome targeting signal type 1 (PTS1) receptor is involved in import of both PTS1 and PTS2: studies with *PEX5*-defective CHO cell mutants. Mol Cell Biol 18:388–399

Shimizu N, Itoh R, Hirono Y, Otera H, Ghaedi K, Tateishi K, Tamura S, Okumoto K, Harano T, Mukai S, Fujiki Y (1999) The peroxin Pex14p: cDNA cloning by functional complementation on a Chinese hamster ovary cell mutant, characterization, and functional analysis. J Biol Chem 274:12593–12604

Shimozawa N, Suzuki Y, Zhang Z, Imamura A, Toyama R, Mukai S, Fujiki Y, Tsukamoto T, Osumi T, Orii T, Wanders RJA, Kondo N (1999) Nonsense and temperature-sensitive mutations in *PEX13* are the cause of complementation group H of peroxisome biogenesis disorders. Hum Mol Genet 8: 1077–1083

Shimozawa N, Tsukamoto T, Suzuki Y, Orii T, Fujiki Y (1992) Animal cell mutants represent two complementation groups of peroxisome-defective Zellweger syndrome. J Clin Invest 90:1864–1870

Tamura S, Matsumoto N, Imamura A, Shimozawa N, Suzuki Y, Kondo N, Fujiki Y (2001) Phenotype-genotype relationships in peroxisome biogenesis disorders of *PEX1*-defective complementation group 1 are defined by Pex1p-Pex6p interaction. Biochem J 357:417–426

Tamura S, Okumoto K, Toyama R, Shimozawa N, Tsukamoto T, Suzuki Y, Osumi T, Kondo N, Fujiki Y (1998) Human *PEX1* cloned by functional complementation on a CHO cell mutant is responsible for peroxisome-deficient Zellweger syndrome of complementation group I. Proc Natl Acad Sci USA 95:4350–4355

Tsukamoto T, Yokota S, Fujiki Y (1990) Isolation and characterization of Chinese hamster ovary cell mutants defective in assembly of peroxisomes. J Cell Biol 110:651–660

van den Bosch H, Schutgens RBH, Wanders RJA, Tager JM (1992) Biochemistry of peroxisomes. Annu Rev Biochem 61:157–197

Walter C, Gootjes J, Mooijer PA, Portsteffen H, Klein C, Waterham HR, Barth PG, Epplen JT, Kunau W-H, Wanders RJA, Dodt G (2001) Disorders of peroxisome biogenesis due to mutations in *PEX1:* phenotypes and PEX1 protein levels. Am J Hum Genet 69:35–48

Yahraus T, Braverman N, Dodt G, Kalish JE, Morrell JC, Moser HW, Valle D, Gould SJ (1996) The peroxisome biogenesis disorder group 4 gene, *PXAAA1,* encodes a cytoplasmic ATPase required for stability of the PTS1 receptor. EMBO J 15:2914–2923

Yanago E, Hiromasa T, Matsumura T, Kinoshita N, Fujiki Y (2002) Isolation of Chinese hamster ovary cell *pex* mutants: two *PEX7*-defective mutants. Biochem Biophys Res Commun 293:225–230